



ARL-RP-0548 • SEP 2015



# Fuel Effects on Nozzle Flow and Spray Using Fully Coupled Eulerian Simulations

by Luis Bravo, Qingluan Xue, Sibendu Som,  
Christopher Powell, and Chol-Bum M Kweon

Reprinted from the Proceedings of the ASME Power Conference. ASME 2015; 2015 Jun 28–Jul 2; San Diego, CA.

Approved for public release; distribution is unlimited.

## **NOTICES**

### **Disclaimers**

The findings in this report are not to be construed as an official Department of the Army position unless so designated by other authorized documents.

Citation of manufacturer's or trade names does not constitute an official endorsement or approval of the use thereof.

Destroy this report when it is no longer needed. Do not return it to the originator.



# **Fuel Effects on Nozzle Flow and Spray Using Fully Coupled Eulerian Simulations**

**by Luis Bravo and Chol-Bum M Kweon**  
*Vehicle Technology Directorate, ARL*

**Qingluan Xue, Sibendu Som, and Christopher Powell**  
*Argonne National Laboratory, Argonne, IL*

Reprinted from the Proceedings of the ASME Power Conference. ASME 2015; 2015 Jun 28–Jul 2; San Diego, CA.

REPORT DOCUMENTATION PAGE				Form Approved OMB No. 0704-0188	
<p>Public reporting burden for this collection of information is estimated to average 1 hour per response, including the time for reviewing instructions, searching existing data sources, gathering and maintaining the data needed, and completing and reviewing the collection information. Send comments regarding this burden estimate or any other aspect of this collection of information, including suggestions for reducing the burden, to Department of Defense, Washington Headquarters Services, Directorate for Information Operations and Reports (0704-0188), 1215 Jefferson Davis Highway, Suite 1204, Arlington, VA 22202-4302. Respondents should be aware that notwithstanding any other provision of law, no person shall be subject to any penalty for failing to comply with a collection of information if it does not display a currently valid OMB control number.</p> <p><b>PLEASE DO NOT RETURN YOUR FORM TO THE ABOVE ADDRESS.</b></p>					
1. REPORT DATE (DD-MM-YYYY) September 2015		2. REPORT TYPE Reprint		3. DATES COVERED (From - To) October 2014–June 2015	
4. TITLE AND SUBTITLE Fuel Effects on Nozzle Flow and Spray Using Fully Coupled Eulerian Simulations				5a. CONTRACT NUMBER	
				5b. GRANT NUMBER	
				5c. PROGRAM ELEMENT NUMBER	
6. AUTHOR(S) Luis Bravo, Qingluan Xue, Christopher Powell, Sibendu Som, and Chol-Bum M Kweon				5d. PROJECT NUMBER	
				5e. TASK NUMBER	
				5f. WORK UNIT NUMBER	
7. PERFORMING ORGANIZATION NAME(S) AND ADDRESS(ES) US Army Research Laboratory ATTN: RDRL-VTP Aberdeen Proving Ground, MD 21005-5066				8. PERFORMING ORGANIZATION REPORT NUMBER ARL-RP-0548	
9. SPONSORING/MONITORING AGENCY NAME(S) AND ADDRESS(ES)				10. SPONSOR/MONITOR'S ACRONYM(S)	
				11. SPONSOR/MONITOR'S REPORT NUMBER(S)	
12. DISTRIBUTION/AVAILABILITY STATEMENT Approved for public release; distribution is unlimited.					
13. SUPPLEMENTARY NOTES Reprinted from the Proceedings of the ASME Power Conference. ASME 2015; 2015 Jun 28–Jul 2; San Diego, CA.					
14. ABSTRACT The objective of this study is to examine the impact of single and multi-component surrogate fuel mixtures on the atomization and mixing characteristics of non-reacting isothermal diesel engine sprays. An Eulerian modeling approach was adopted to simulate both the internal nozzle flow dynamics and the emerging turbulent spray in the near nozzle region in a fully-coupled manner. The Volume of Fluids (VoF) methodology was utilized to treat the two-phase flow dynamics including a Homogenous Relaxation approach to account for nozzle cavitation effects. To enable accurate simulations, the nozzle geometry and in-situ multi-dimensional needle lift and off-axis motion profiles have been characterized via the X-ray phase-contrast technique at Argonne National Laboratory. The flow turbulence is treated via the classical $k-\epsilon$ Reynolds Average Navier Stoke (RANS) model with in-nozzle and near field resolution of 30 $\mu\text{m}$ . Several multi-component surrogate mixtures were implemented using linear blending rules to examine the behavior of petroleum, and alternative fuels including: JP-8, JP-5, Hydro-treated Renewable Jet (HRJ), Iso-Paraffinic Kerosene (IPK) with comparison to single- component n-dodecane fuel on ECN Spray A nozzle spray dynamics. The results were validated using transient rate-of- injection measurements from the Army Research Laboratory at Spray A conditions as well as projected density fields obtained from the line-of-sight measurements from X-ray radiography measurements at The Advanced Photon Source at Argonne National Laboratory. The conditions correspond to injection pressure, nominal fuel temperature, and ambient density of 1500 bar, 363 K, and 22.8 $\text{kg/m}^3$ , respectively. The simulation results provide a unique high-fidelity contribution to the effects of fuels on the spray mixing dynamics. The results can lead to improvements in fuel mixture distributions enhancing performance of military vehicles.					
15. SUBJECT TERMS surrogate fuel, turbulence, spray, diesel, X-ray					
16. SECURITY CLASSIFICATION OF:			17. LIMITATION OF ABSTRACT UU	18. NUMBER OF PAGES 16	19a. NAME OF RESPONSIBLE PERSON Luis Bravo
a. REPORT Unclassified	b. ABSTRACT Unclassified	c. THIS PAGE Unclassified			19b. TELEPHONE NUMBER (Include area code) 410-278-9525

## Power 2015-49554

### FUEL EFFECTS ON NOZZLE FLOW AND SPRAY USING FULLY COUPLED EULERIAN SIMULATIONS

**Luis Bravo**

U.S. Army Research Laboratory  
Aberdeen Proving Ground, MD

**Qingluan Xue**

Argonne National Laboratory  
Argonne, Ill

**Sibendu Som**

Argonne National Laboratory  
Argonne, Ill

**Christopher Powell**

Argonne National Laboratory  
Argonne, Ill

**Chol-Bum M. Kweon**

U.S. Army Research Laboratory  
Aberdeen Proving Ground, MD

#### ABSTRACT

The objective of this study is to examine the impact of single and multi-component surrogate fuel mixtures on the atomization and mixing characteristics of non-reacting isothermal diesel engine sprays. An Eulerian modeling approach was adopted to simulate both the internal nozzle flow dynamics and the emerging turbulent spray in the near nozzle region in a fully-coupled manner. The Volume of Fluids (VoF) methodology was utilized to treat the two-phase flow dynamics including a Homogenous Relaxation approach to account for nozzle cavitation effects. To enable accurate simulations, the nozzle geometry and in-situ multi-dimensional needle lift and off-axis motion profiles have been characterized via the X-ray phase-contrast technique at Argonne National Laboratory. The flow turbulence is treated via the classical  $k - \epsilon$  Reynolds Average Navier Stoke (RANS) model with in-nozzle and near field resolution of 30  $\mu\text{m}$ . Several multi-component surrogate mixtures were implemented using linear blending rules to examine the behavior of petroleum, and alternative fuels including: JP-8, JP-5, Hydro-treated Renewable Jet (HRJ), Iso-Paraffinic Kerosene (IPK) with comparison to single-component n-dodecane fuel on ECN Spray A nozzle spray dynamics. The results were validated using transient rate-of-injection measurements from the Army Research Laboratory at Spray A conditions as well as projected density fields obtained from the line-of-sight measurements from X-ray radiography measurements at The Advanced Photon Source at Argonne National Laboratory. The conditions correspond to injection pressure, nominal fuel temperature, and ambient density of 1500 bar, 363 K, and 22.8  $\text{kg/m}^3$ , respectively. The simulation results provide a unique high-fidelity contribution to the effects of fuels on the spray mixing dynamics. The results can lead to improvements in fuel mixture distributions enhancing performance of military vehicles.

#### NOMENCLATURE

$M$	= Projected density, $\text{ug/mm}^2$
$TIM$	= Total Integrated Mass, $\text{ug/mm}$
$d_o$	= Nozzle diameter, $\mu\text{m}$
$x$	= Axial distance from nozzle, $\text{mm}$
$y$	= Transverse distance from nozzle, $\text{mm}$
$\rho_f$	= Density of liquid fuel, $\text{kg/m}^3$
$\rho_a$	= Density of ambient gas, $\text{kg/m}^3$
$VOF$	= Volume of Fluid model
$\alpha$	= Volume of Fluid Scalar
$ROI$	= Rate of Injection, $\text{mg/ms}$
$HRJ$	= Hydro-treated Renewable Jet Fuel
$IPK$	= Iso-paraffinic Kerosene Jet Fuel
$JP-8$	= Jet Propellant 8
$JP-5$	= Jet Propellant 5
$CFD$	= Computational Fluid Dynamics
$RANS$	= Reynolds Average Navier Stokes
$ARL$	= Army Research Laboratory
$AMR$	= Adaptive Mesh Refinement
$MPI$	= Message Protocol Interface
$PISO$	= Pressure Implicit Split Operator
$ANL$	= Argonne National Laboratory
$ECN$	= Engine Combustion Network
$EDM$	= Electric Discharge Machining
$ASOI$	= After Start of Injection

## INTRODUCTION

An important factor in direct injection engines is characterizing the spray mixture formation process. Improvements in the air-fuel mixing can lead to a leaner combustion process resulting in enhanced engine efficiencies and improved performance. The spray mixing characteristics can be strongly influenced by the fuel's physical properties i.e., volatility, viscosity, and surface tension. These properties are largely dependent on the fuel chemical composition and the hydrogen to carbon ratio. Petroleum-based fuels are chemically complex typically containing thousands of components. Large variations in petroleum derived fuel composition have been reported arising from individual refinery processes, crude oil source, and also varying with season, year and age of the fuel. This myriad of complex factors makes it difficult to control the consistency of the fuel composition for research purposes. As a result, surrogate fuels are desirable for experimental and computational tractability and reproducibility. Surrogate fuels have typically been developed to represent physical or chemical properties and are particularly useful in numerical simulations since it simplifies the description of the fuel composition while reducing the computational cost burden. The importance of surrogate fuels in research (experiments and modeling) has been emphasized through the launching of a large workshop named *Surrogate Fuels Working Group* to bring forward a consensus on the development of databases for real transportation fuels (1). As a result, the jet-fuel (also gasoline, and diesel) working group has provided a palette of compounds from which to construct surrogate fuel mixtures; several of the existing surrogates have also been presented and compared to experimental data (2–11).

Previous numerical works have focused on developing the chemical-kinetic models describing select aspects of kerosene spray behavior. Earlier works by Schultz et al. (2) proposed a 12-component surrogate mixtures which has led to further developments of mixtures for various applications. The work by Edwards et al. (3) have reviewed several surrogate fuels and targeted validations with various applications. It was noted that fuel injection, vaporization, and mixing should use a multi-component mixture where the distillation curve is a critical parameter. Bravo et al. (4) carried out high-fidelity non-reacting spray simulations and has shown the suitability of several multi-component kerosene surrogates at diesel engine conditions. The measurements were validated with the Army Research Laboratory (ARL) evaporating spray measurements of Kurman et al. (5) demonstrating good agreement for several fuel injector configurations. Under reacting conditions, Violi et al. (6) presented a surrogate mixture of six pure hydrocarbon (Utah surrogate) and found that it correctly simulated the distillation characteristics of JP-8. Their work was validated with laminar premixed flames burning kerosene. Similarly, Montgomery et al. (7) developed a reduced four component mixture mechanism with reasonable agreement to a detailed 12 component surrogate and ignition delay measurements. More recently, Humer et al. (8) introduced three additional surrogates

composed of key reference fuels denoted as surrogates A, B, and C, respectively. The counterflow configuration was employed for validation with experiments where the predictions of critical conditions of extinction and auto-ignition for surrogates were in good agreements with jet fuel data. Note that Honnet et al. (9) also introduced a widely used kerosene surrogate for JP-8, the Aachen surrogate. This two component mixture was targeted at reproducing critical conditions in addition to volume soot fraction measured in laminar non-premixed flows. This also provided an enhanced chemical mechanism for the combustion process and was validated with a wide set of data from shock tubes, rapid compression machines, jet stirred reactors, burner stabilized premixed flames and freely propagating premixed flame. Encouraging results were obtained with respect to the non-premixed combustion of kerosene. It is important to note that until recently surrogate mixtures have not been validated in detail numerically for non-reacting spray applications with military and alternative fuels at diesel like engine conditions.

Recent developments in X-ray radiography at The Advanced Photon Source at Argonne National Laboratory (ANL) have provided unique measurements of the spray structure in the near nozzle field (10-20 mm). Kastengren et al. (13) presented measured projected mass density fields in diesel type jets at various operating conditions demonstrating the asymmetries in fuel mass distributions. The asymmetries were reported to arise from the manufacturing eccentricities leading to imperfections in the injector nozzle geometry (i.e., non-axial nozzle exit) (14). Similar studies have also measured the internal transient geometry and motion of the injector nozzle, needle valve and hydraulics (14). These findings have sparked interest in spray modeling work which couples the transient needle motion with the internal flow dynamics and ensuing spray. The works by Xue et al. (15-16) have integrated this in an Eulerian modeling approach using a single-component reference fuel and reported on the effect of needle wobble on spray dynamics at engine like conditions. The work also includes validations with X-ray radiography projected density fields and measured mass-flow-rates profiles with good agreement (16).

In this work, a group of surrogate fuels have been selected to investigate the mixing properties of non-reacting heavy fuel sprays. A unique Eulerian 3D Computational Fluid Dynamics (CFD) spray modeling approach is adopted to model the atomization and mixing process. A Reynolds-Averaged Navier Stokes (RANS) simulation turbulence modeling approach is prescribed in addition to the single-fluid mixture model based Volume of Fluids (VOF) approach for the two-phase flow analysis. The ARL experimental dataset corresponding to fuel injector analyzer measurements, is utilized for validation purposes on the nozzle mass flow rates i.e., Rate-of-Injection (ROI). Also note that the surrogate physical properties have been implemented for the numerical studies. Note that a principal objective of the current work is to establish the suitability of proposed surrogate mixtures that have the similar

physical and chemical properties as of a practical, petroleum-derived and alternative fuels, in particular, the mixing jet behavior at diesel like conditions. This validation is necessary, as it will serve as guidance to future evaporating non-reacting and reacting engine spray simulations.

## NUMERICAL METHOD

The multi-dimensional CONVERGE CFD solver (17) has been adopted in this study to perform the detailed Eulerian spray simulations. The software is a compressible Navier Stokes solver which is based on a first order predictor-corrector time integration scheme, and a choice of second or higher order finite volume schemes for spatial discretization. It features a non-staggered, collocated, computation grid framework utilizing a Rhie-Chow interpolation technique to avoid spurious oscillations. An efficient geometric multi-grid treatment is used to solve the pressure equation, and parallel computing is based on implementation of Message Passing Interface (MPI) protocol. It provides the option of increasing resolution locally through static fixed-grid embedding, and dynamically through Adaptive Mesh Refinement (AMR) activated through user specified criteria. The solver also provides a choice between a number of modeling options for the treatment of turbulence including advanced Large Eddy Simulation (LES) and Reynolds-Averaged Navier-Stokes (RANS) models.

The Eulerian formulation adopted in this study describes the ambient gas and liquid fuel as a single fluid mixture using the Favre Averaged Navier Stokes Equations while adopting a traditional RANS modeling (18-19) approach. The compressible system of transport equations for mass, and momentum are presented here,

$$\frac{\partial \bar{\rho}}{\partial t} + \frac{\partial \bar{\rho} \tilde{u}_j}{\partial x_j} = 0 \quad (1)$$

$$\frac{\partial \bar{\rho} \tilde{u}_i}{\partial t} + \frac{\partial \bar{\rho} \tilde{u}_i \tilde{u}_j}{\partial x_j} = -\frac{\partial \bar{P}}{\partial x_i} + \frac{\partial \bar{\sigma}_{ij}}{\partial x_j} - \frac{\partial \tau_{ij}}{\partial x_j} \quad (2)$$

where  $\sigma_{ij}$  and  $\tau_{ij}$  are the viscous and modeled Reynolds stress tensor. The viscous stress is modeled using the Boussinesq eddy viscosity method with  $\delta_{ij}$  as the Kronecker delta,

$$\tau_{ij} = \mu_t \left( \frac{\partial \tilde{u}_i}{\partial x_j} + \frac{\partial \tilde{u}_j}{\partial x_i} - \frac{2}{3} \frac{\partial \tilde{u}_k}{\partial x_k} \delta_{ij} \right) - \frac{2}{3} \bar{\rho} k \delta_{ij} \quad (3)$$

A standard  $k - \epsilon$  RANS model is used to as follows,

$$\mu_t = \bar{\rho} C_\mu \frac{k}{\epsilon} \quad (4)$$

With the turbulent kinetic energy, dissipation and energy equations as,

$$\frac{\partial \bar{\rho} k}{\partial t} + \frac{\partial \bar{\rho} \tilde{u}_i k}{\partial x_i} = \tau_{ij} \frac{\partial \tilde{u}_i}{\partial x_j} + \frac{\partial}{\partial x_j} \left( \frac{\mu_t}{Pr_{tke}} \frac{\partial k}{\partial x_j} \right) - \bar{\rho} \epsilon \quad (5)$$

$$\begin{aligned} \frac{\partial \bar{\rho} \epsilon}{\partial t} + \frac{\partial \bar{\rho} \tilde{u}_i \epsilon}{\partial x_i} = & \frac{\partial}{\partial x_j} \left( \frac{\mu_t}{Pr_{tke}} \frac{\partial \epsilon}{\partial x_j} \right) - C_3 \bar{\rho} \epsilon \frac{\partial \tilde{u}}{\partial x_i} \\ & + \left( C_{\epsilon 1} \frac{\partial \tilde{u}_i}{\partial x_j} \tau_{ij} - C_{\epsilon 2} \bar{\rho} \epsilon \right) \frac{\epsilon}{k} - \bar{\rho} R \end{aligned} \quad (6)$$

The  $R$  parameter is a function of turbulence model constants for the RANS model. Their values in this study are  $C_{\epsilon 1} = 1.60$ ,  $C_{\epsilon 2} = 1.92$ , and  $C_{\epsilon 3} = -1.0$ .

$$\begin{aligned} \frac{\partial \bar{\rho} \tilde{e}}{\partial t} + \frac{\partial \bar{\rho} \tilde{u}_i \tilde{e}}{\partial x_i} = & -\bar{p} \frac{\partial \tilde{u}_i}{\partial x_i} + \tau_{ij} \frac{\partial \tilde{u}_i}{\partial x_j} + \frac{\partial}{\partial x_i} \left( K \frac{\partial \tilde{T}}{\partial x_i} \right) \\ & + \frac{\partial}{\partial x_j} \left( \bar{\rho} D_t \sum \tilde{h}_m \frac{\partial \tilde{u}_i}{\partial x_j} \right) \end{aligned} \quad (7)$$

In the above  $K$ ,  $\tilde{T}$ ,  $D_t$ ,  $\tilde{h}_m$ , are conductivity, turbulent diffusion, gas temperature, and enthalpy of species of the mixture.

The fuel mass fraction description follows,

$$\frac{\partial \bar{\rho} \tilde{Y}}{\partial t} + \frac{\partial \bar{\rho} \tilde{u}_i \tilde{Y}}{\partial x_i} = -\frac{\partial \bar{\rho} \tilde{u}_i \tilde{Y}'}{\partial x_i} - \rho Y_{evap} \quad (8)$$

with  $u'_i$  and  $Y'$  representing fluctuations in velocity and liquid fuel mass fraction, and  $\rho Y_{evap}$  representing an evaporation source term which is negligible for the present non-evaporating conditions. The closure for the liquid mass transport term  $\bar{\rho} \tilde{u}_i \tilde{Y}'$  is based on a turbulent gradient flux model (18),

$$\bar{\rho} \tilde{u}_i \tilde{Y}' = \frac{\mu_t}{Sc_t} \frac{\partial \tilde{Y}}{\partial x_i} \quad (9)$$

Where  $\mu_t = 0.7$ . The averaged density of the immiscible two phase mixture is given by,

$$\frac{1}{\bar{\rho}} = \frac{\tilde{Y}}{\bar{\rho}_l} + \frac{1 - \tilde{Y}}{\bar{\rho}_g} \quad (10)$$

where gas density is prescribed through an equation of state  $\bar{\rho}_g = \bar{p}/(R_g \tilde{T})$  while assuming the liquid phase density to be constant. It is important to note that multi-component mixture properties are prescribed through weighted average property values from the surrogate blend mass fraction distributions.

The VOF Eulerian method used for the two-phase flow analysis is based on the volume fraction scalar( $\alpha$ ). It is defined as follows,

$$\alpha = \begin{cases} 0 & \text{cell is filled with pure liquid} \\ 1 & \text{cell is filled with pure gas} \end{cases}$$

Intermediate values between  $0 < \alpha < 1$  represent a mixture of liquid and gas. In the current study, the volume fraction is directly extracted from the fuel mass fraction transport equation (8) and the bulk value of mass-densities as follows,

$$\alpha = \frac{(1 - \tilde{Y})/\bar{\rho}_g}{(1 - \tilde{Y})/\bar{\rho}_g + \tilde{Y}/\bar{\rho}_l} \quad (11)$$

For time advancement, equations (1) and (2) are solved numerically using a classical predictor-corrector scheme in which the velocity field is first integrated using the Navier Stokes equation (2) and then corrected to enforce mass conservation (1), using a modified pressure value. This is achieved using the modified Pressure Implicit with Splitting of Operator (PISO) algorithm first introduced by Issa (12).

## EXPERIMENTS FOR COMPARISON

Two datasets of measurements were utilized in this study for validation purposes. The first dataset corresponds to Argonne National Laboratory (ANL) X-ray radiography measurements of spray projected density, nozzle geometry, and needle displacement for single-component n-dodecane fuel (20). Note the projected density field measurements are presented as ensemble averaged fields over multiple shots. The table below shows the experimental conditions:

Table1. Conditions for non-evaporating Spray A X-ray radiography measurement (21).

Ambient gas temperature	303 (K)
Ambient gas pressure	2.0 (MPa)
Ambient gas density	22.8 (kg/m <sup>3</sup> )
Ambient gas N <sub>2</sub>	100%
Nozzle K factor	1.5
Nozzle outlet diameter	0.090 mm
Number of holes	single-hole
Fuel injection pressure	150 (MPa)
Fuel	n-dodecane
Fuel temperature at nozzle	343 K
Injection duration	1.5 (ms)
Injected mass	3.5 (mg)

The second dataset was conducted at the ARL using a common-rail fuel injector, IAV injection analyzer, for nozzle mass-flow-rates, i.e., Rate-of-Injection, measurements of JP-8 and IPK fuels. It is important to note that ROI profiles are also averaged over 100 shots each reducing the effects of outliers in the signal. The measurement details for this study are provided below,

Table2. Conditions for nozzle-flow dataset ROI measurements with various fuels.

Injector type	BOSCH CRIN3
Number of holes	single-hole
Fuels	n-dodecane, JP-8, IPK
Fuel injection pressure	150 (MPa)
Nozzle K factor (nominal)	1.5
Nozzle outlet diameter	0.090 mm
Injection duration (nominal)	1.5 (ms)

## COMPUTATIONAL SETUP

Three-dimensional simulations have been conducted using a single-mixture VOF model that couples the needle motion with the ensuing spray. The nozzle tip injector, sac, and needle geometry have been utilized in the simulations via the characterization obtained from the Engine Combustion Network (ECN) community via high-resolution X-ray measurements. Figure 1, shows the characterization of needle valve motion obtained from (20).

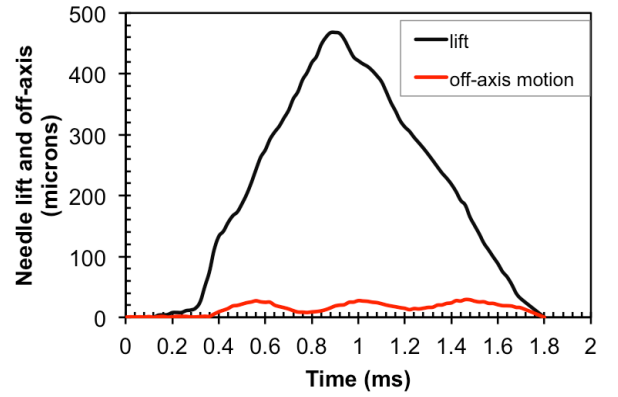


Figure 1. Spray-A Injector characterization. Needle lift and off-axis measurements.

The transient needle lift shown along the y-axis in the figure prescribes most of the injected fuel mass in the ROI measurements. The off-axis motion results in needle wobble in the transverse and span-wise flow directions. The needle profiles are prescribed as dynamic boundary conditions (immersed) in the simulation work.

The spray chamber region in the simulations (cylindrical) has dimensions of 50 mm by 200 mm in diameter and length respectively. Fixed embedding is prescribed in the near nozzle region with a base grid size of 2 mm. Figure 2a shows a fuel mixture distribution for IPK at  $t = 0.51$  ms, highlighting the nozzle geometry. Figure 2b shows a close inspection of the injector nozzle with the cell distribution and fixed embedding regions. Figure 2b also shows the misalignment of the orifice in the sac arising from the manufacturing eccentricities.

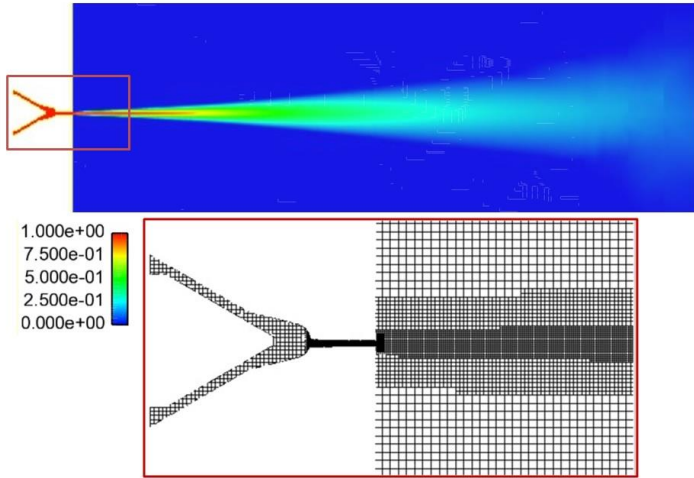


Figure 2. Coupled spray solution and mesh. (a) Fuel mixture fraction distribution, and (b) zoomed view of the mesh in nozzle and outflow regions.

From previous simulation studies it was concluded that a grid-size of  $30\ \mu\text{m}$  (nozzle diameter to cell size ratio of 3) would be sufficient to capture the important spray features (16). This recommendation is based on a trade-off between accuracy and computational cost. Note also, each simulation was run on 32 processors with peak cell counts of  $\sim 850,000$  and total wall-clock time of 128 hours running on CRAY XE6 Linux architectures. The resolution is embedded inside the nozzle orifice and up to 2 mm axially in the spray region. The surrogate components for each fuel are listed in Table 3 in molar fraction.

## RESULTS AND DISCUSSIONS

The Eulerian VOF simulations were carried out and inspected using a resolution of  $30\ \mu\text{m}$  in the nozzle and optically dense spray regions. A single RANS realization of the mean flow field was obtained for each of the single and multi-component fuels considered. The fuel distributions are compared using the projected mass density from the simulations. Note that experimentally this is obtained from a line-of-sight integration along the x-Ray beam. To enable one-to-one comparison a similar procedure was implemented while post-processing the simulation results.

Table 3. Surrogate components and its blend density at 300K

Fuel	Surrogate component (mole fraction)							Surrogate blend density ( $\text{kg/m}^3$ )
	Hexadecane	Iso-dodecane	m-Xylene	Butyl cyclohexane	n-Propyl benzene	Decane	Trimethyl-Benzene	
JP5	0.53	0.15	0.24	0.08	0.0	0.0	0.0	790
HRJ	0.65	0.33	0.0	0.0	0.02	0.0	0.0	762
IPK	0.21	0.65	0.0	0.12	0.02	0.0	0.0	758
JP8	0.0	0.0	0.0	0.0	0.0	0.83	0.17	756

## TRANSIENT RESULTS

The projected mass density simulation results below compare the influence of density variations in single and multi-component surrogate mixtures. The solution corresponds to an early integration time of  $t = 0.025\ \text{ms}$ . It is apparent that each surrogate fuel has a specific and characteristic mixture distribution. Note the peak penetration lengths for IPK and JP-8 occur at  $8.8\ \text{mm}$  and  $8.9\ \text{mm}$ , respectively with density values of  $M = 25\ \mu\text{g/mm}^2$ . Although n-dodecane, HRJ and JP-5 have similar peak penetration values  $\sim 6.8\ \text{mm}$ , it is clear that the spray structure is different as indicated from the dispersion and spray tip characteristics.

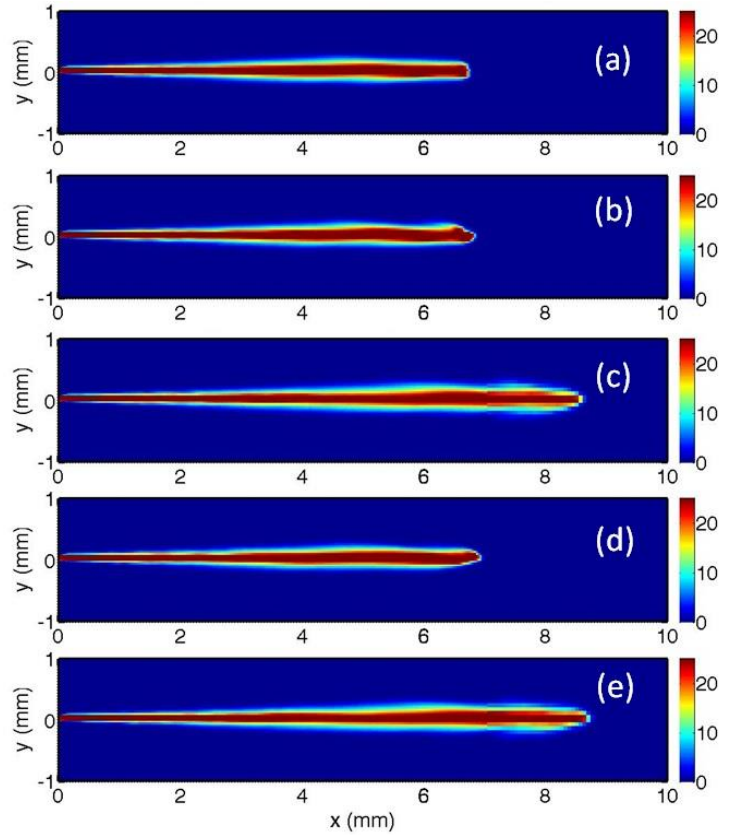


Figure 3. Contours of projected mass density ( $M$ ) distributions ( $\mu\text{g/mm}^2$ ), at  $0.025\ \text{ms}$  ASOI from simulations with various fuel mixtures: (a) n-dodecane (b) HRJ (c) IPK (d) JP-5 (e) JP-8.

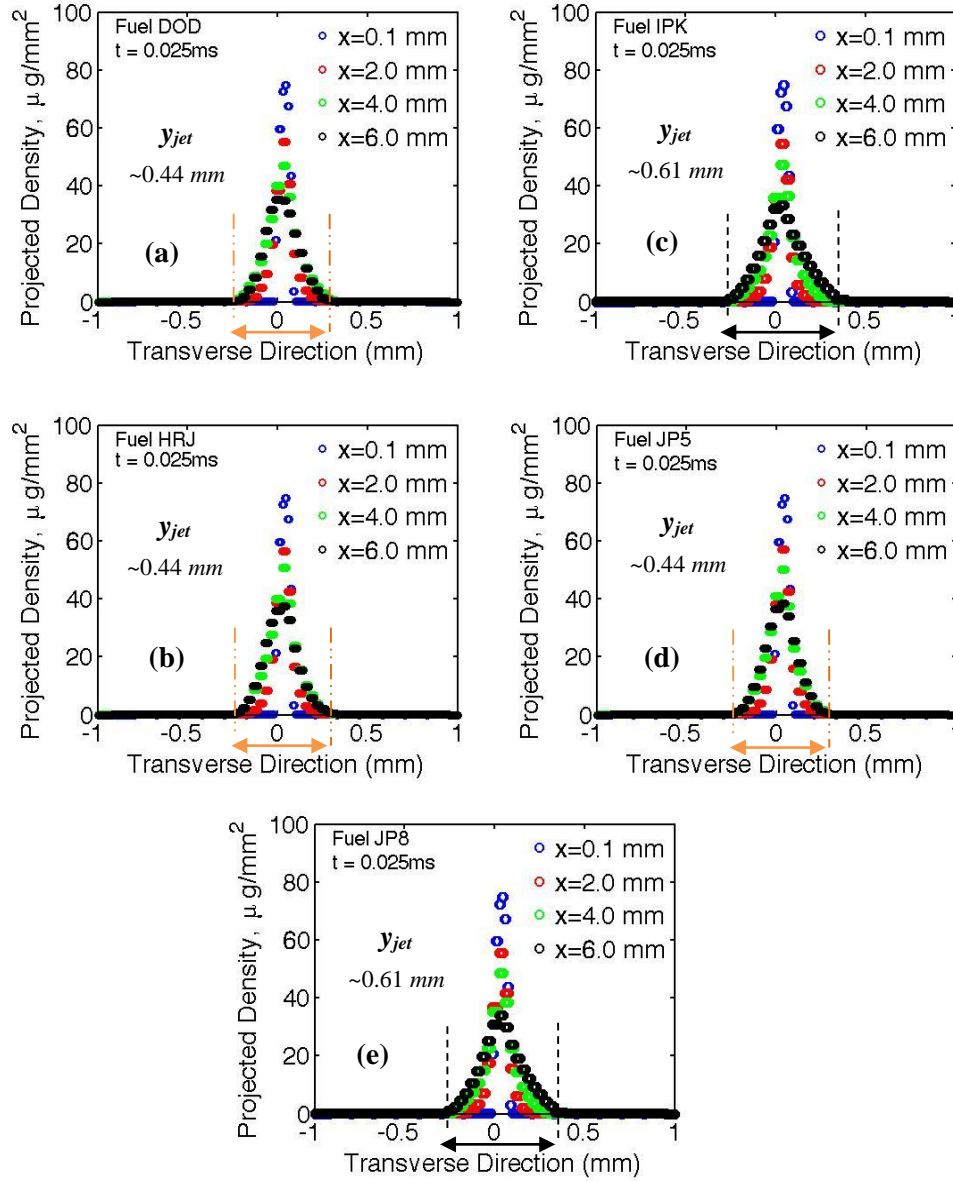


Figure 4. Transverse profiles of projected mass density ( $M$ ) at 4 axial stations  $\{x = 0.1, 2.0, 4.0, 6.0 \text{ mm}\}$  in the spray downstream direction at  $t = 0.025 \text{ ms}$ . The surrogate mixtures considered correspond to (a) n-dodecane (b) HRJ (c) IPK (d) JP-5 and (e) JP-8.

Figure 4 presents transverse profile of the projected density at several locations  $\{x = 0.1, 2.0, 4.0, 6.0 \text{ mm}\}$  downstream of the nozzle. It is apparent that each transverse profile is asymmetric arising from the manufacturing discrepancies in the real nozzle geometry. The projected density profiles follow a typical power law  $M \sim M_o x^{-n}$  accounting for the decay in its peak magnitude with axial direction (where  $M_o$  is an initial value and  $n$  is a power constant). The jet profiles also increase in width with axial direction due to the natural increased mixing, i.e., air entrainment, in the radial direction. Note the jet width, as indicated by the zero intercept of the profiles at  $x = 6.0 \text{ mm}$ , has a value of  $y_{jet} \sim 0.6 \text{ mm}$  for IPK and JP-8 mixtures. This is 1.5 times larger than the findings for n-dodecane, HRJ, and JP-5 with similar widths at  $y_{jet} \sim 0.44 \text{ mm}$  at the present transient conditions. The results suggest that differences in the jet spreading rate arise mainly from blend density variations with lighter fuels typically spreading faster axially and radically than the heavier counterparts (i.e.,  $y_{jet}(JP-8) > y_{jet}(dodecane)$ ).

### STEADY RESULTS

Figure 5 shows steady results obtained at time  $t = 0.51 \text{ ms}$  via contours of projected mass density. The simulations are compared against the X-Ray n-dodecane measurements.

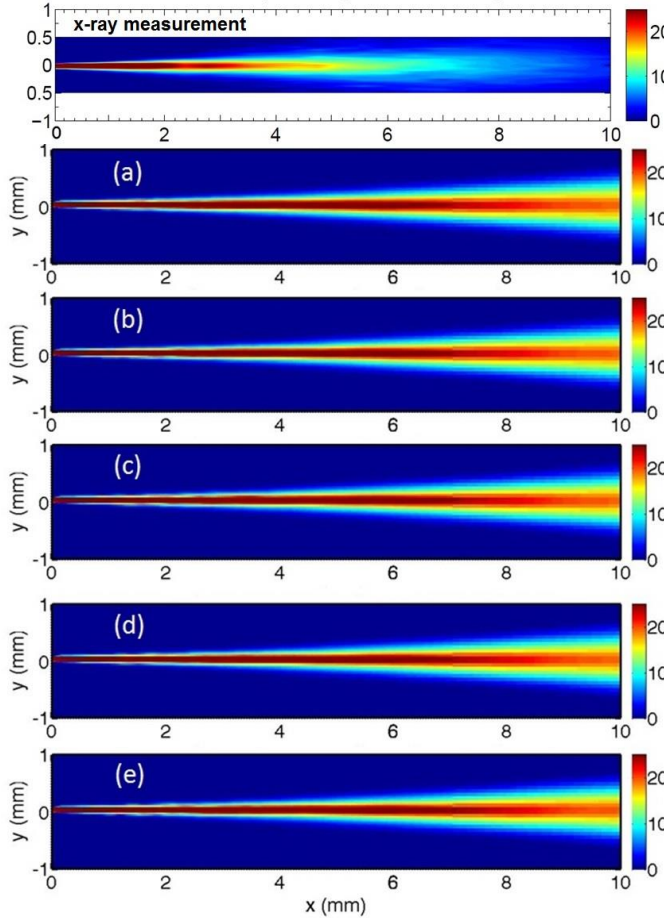


Figure 5. Contours of Projected mass density ( $M$ ) distributions  $\mu\text{g}/\text{mm}^2$ , at 0.51 s ASOI from simulations with various fuel mixtures: (a) n-dodecane (b) HRJ (c) IPK (d) JP-5 (e) JP-8.

At steady conditions, Figure 5 shows insignificant variations with fuel mixtures. Near the axial region upstream  $x = 0-3 \text{ mm}$  the density contours of  $M$  show undulations induced from the off-axis needle motion. Next, the full spray projected density field will be utilized to investigate the Total Integrated Mass (TIM) variations obtained through transverse integration of projected density fields. The projected velocity is calculated as the inverse of TIM, from continuity arguments, and normalized by the peak injection velocity at the nozzle exit.

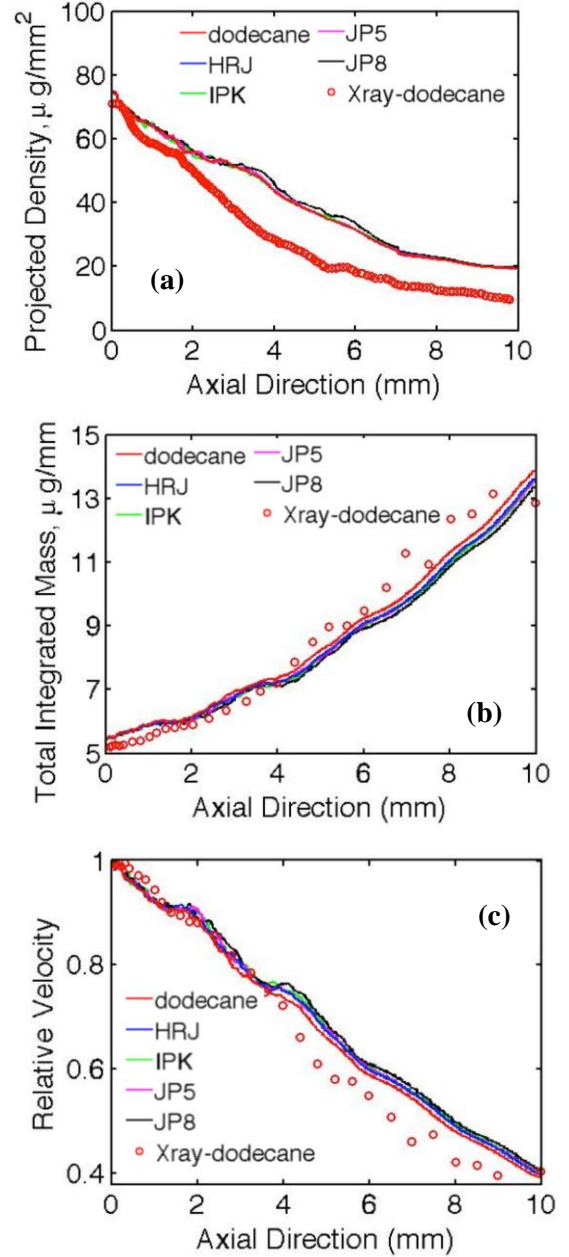


Figure 6. Comparison with X-ray measurements at steady conditions  $t = 0.51 \text{ ms}$  for each fuel considered, (a) projected density in the axial direction,  $\mu\text{g}/\text{mm}^2$  (b) Transverse Integrated Mass, TIM,  $\mu\text{g}/\text{mm}$  (c) Relative Velocity.

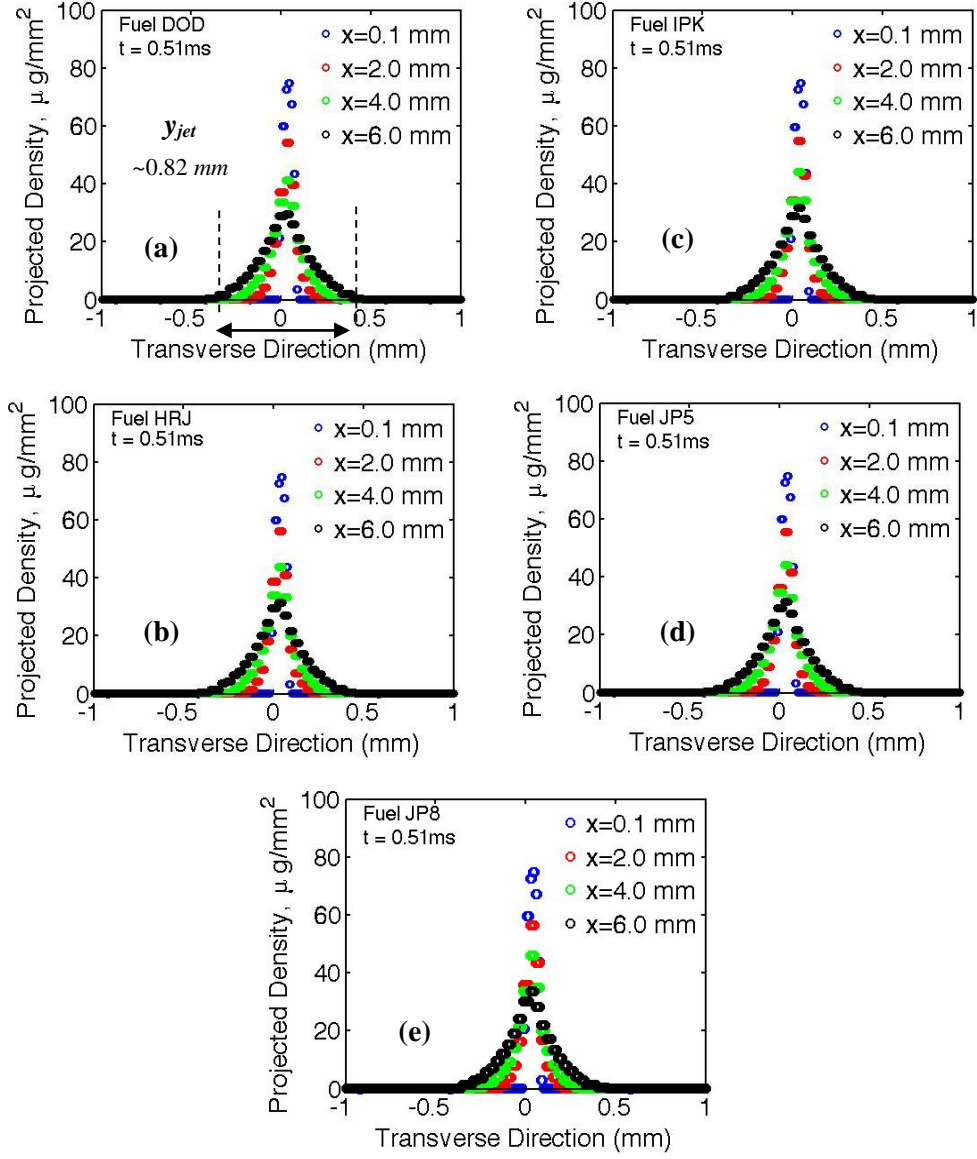


Figure 7. Transverse profiles of projected mass density ( $M$ ) at 4 axial locations  $\{x = 0.1, 2.0, 4.0, 6.0$  mm $\}$  in the spray downstream direction at  $t = 0.51$  ms. The surrogate mixtures considered correspond to (a) n-dodecane (b) HRJ (c) IPK (d) JP-5 and (e) JP-8.

Figure 6a shows the axial development of centerline projected density including the comparison between n-dodecane and the measurements. The model is able to capture the correct trend as in the measurements; however, it is pointed out that an optimization of the parameters (i.e., Schmidt number and turbulence model constants) and higher resolution may be necessary to improve the results. Figure 6a profiles show that lighter multi-component mixture such as JP-8 feature increases in projected density values than the single-component surrogate (n-dodecane) due to their faster spreading rates. The comparisons between Figure 6b-6c with measurements also show good agreements. The variations with different fuels remain subtle; however, it is evident that TIM profiles are larger for single-component heavier fuels decreasing with lighter multi-component mixtures such as JP-8. Similar findings are shown with the relative velocity. Figure 7 depicts the variations of transverse projected density profile with downstream distance  $\{x = 0.1, 2.0, 4.0, 6.0 \text{ mm}\}$  of the spray at  $t = 0.51 \text{ ms}$ . The nominal jet width across all fuel blends is  $y_{jet} \sim 0.82 \text{ mm}$ , in comparison transient profiles report a peak increase of 1.34 in jet width. Note that the variations across all presented fuels will be amplified at higher ambient temperatures due to differences in volatility and vapor pressures of each fuel.

#### NOZZLE MASS FLOW RATES (ROI)

Measured rate-of-injection (ROI) profiles were used as bulk validation parameters for the nozzle flow simulation. As discussed earlier, the fuel injection system consists of a high-pressure fuel bench connected to a common rail system. The high-pressure fuel bench contains a fuel pump operated by an electric motor. For the experiments presented, fuel rail pressure was held constant at 1500 bar following Spray-A specifications, Table 2. The motor speed is maintained by a variable frequency drive. Total energizing times for the presented experiments were  $770 \mu\text{s}$  leading to an injection duration of  $\sim 1.5 \text{ ms}$ . For the single-hole ARL nozzle, all stock 6-holes were welded and an axial orifice was created by an electrical discharging machine (EDM) machining. Each fuel injector was then mapped with an IAV fuel injection analyzer to determine the injected fuel mass and ROI parameters of interest. Note that the analyzer operates on the principle that the fuel mass is related to the speed of sound in the fluid, the cross sectional area of the tube and the wave dynamic pressure as a function of time. ROI signals are ensemble-averaged over 100 realizations to reduce the effects of instantaneous fluctuations.

Figure 8 (a) shows similar behavior across all measured mass flow rates. However, the initial ramping of measured ROI differs between single and multi-component fuels. These variations may be due to the different injector types used in the experiments as the n-dodecane measurements correspond to CRIN2 injector (note SNL measurement technique is different from the ARL injection analyzer. SNL's ROI data overestimates ROI). An indication of this is the consistency between IPK and JP-8 dataset in the ramping region. For all cases, the peak ROI values at steady conditions ( $t = 0.51 \text{ ms}$ ) shows the increasing

trend in peak-injected mass following the same behavior as the CFD counterpart. Figure 8 (b) is a scaled up figure of the ROI simulations showing the impact of physical property variations, in particular the blend fuel density. The trend from larger to smaller ROI values becomes apparent in this figure as the following:  $JP8 > IPK > JP5 > HRJ > \text{dodecane}$  following the surrogate fuel blend prescribed density distributions and in agreements with experiments.

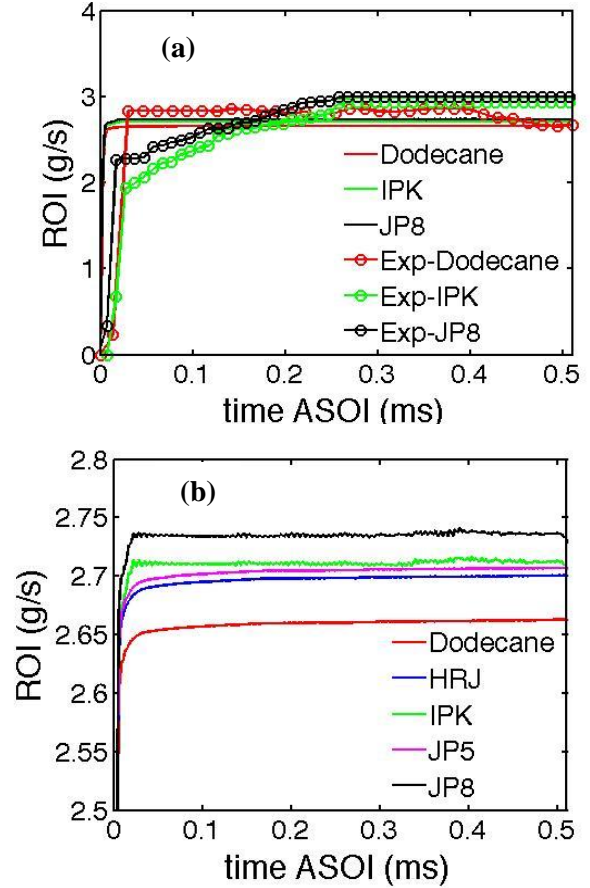


Figure 8. Rate-of-Injection profiles at  $t = 0.51 \text{ ms}$  ASOI from simulations with various fuel mixtures. (a) Comparison of with experiments (b) Highlights of variations in CFD ROI distributions.

At initial time the simulations have a finite needle lift of  $20 \mu\text{m}$  and are started also with liquid filled sac and nozzle hole. This is different from the measurements that may have gas in sac and nozzle flow. Also observe that ROI simulation signals show evidence of oscillations across all fuels. This can be a result of presenting single-realization simulation, as some of the fluctuations will be damped through averaging of additional events.

#### CONCLUSIONS

Three-dimensional numerical simulations of engine sprays have been conducted using a compressible VOF single mixture

formulation to treat the multiphase flow. The simulation geometry includes transient needle displacements, sac volume, and the nozzle tapered channel. The asymmetries are evident in the geometry as was demonstrated in Figure 2. The fuels considered in this study correspond to practical petroleum and alternative fuels including n-dodecane, HRJ, IPK, JP-5 and JP-8. Single and multi-component surrogate mixtures have been selected for their representation as presented earlier. The following observations are summarized:

- RANS simulation results are adequate in capturing the spray injector transients in jet width dispersion and fuel mass density distributions. The simulations compare well with the nozzle and ensuing spray presented measurements.
- Transient results of projected density indicate that spreading rate is highly depended on fuel blend mass density distributions. Jet widths for IPK and JP-8 ( $y_{jet} \sim 0.61 \text{ mm}$ ) mixture were found to be 1.5 times larger than n-dodecane, HRJ, and JP-5 ( $y_{jet} \sim 0.44 \text{ mm}$ ).
- The differences in steady state results of projected density are less pronounced than their transient counterpart for different fuels. The nominal jet width across fuel blends ( $y_{jet} \sim 0.82 \text{ mm}$ ) was reported to be 1.3 times larger than peak transient profiles ( $y_{jet} \sim 0.61 \text{ mm}$ ). At steady conditions, variations in projected density, TIM and relative velocity consistently show the influence of higher blend density on solution.
- ROI simulations capture the correct physical behavior when compared to experiments. The simulations show higher injection rates for lighter fuel blends with good agreements. ROI signals also show natural oscillations arising from traveling pressure waves inside the nozzle flow.

The results present successful simulations of internal nozzle flow in a single-hole injector with attention to surrogate mixtures. Future works will include extending the present set of results to higher ambient temperature and pressures (typical engine operating ambient conditions are 850-950 K and 40-80 bar) while keeping the fuel-to-air density ratio constant. It is expected that evaporation effects will have a strong impact on projected density, dispersion, and jet width characteristics. Since X-ray diagnostics are not yet performed under high-temperature conditions and optical diagnostics cannot provide the above mentioned details, CFD simulations may be the key tool in further understanding differences in mixing and combustion characteristics of single and multi-component fuels.

## ACKNOWLEDGMENTS

This work was supported in part by high performance computer time and resources from the DoD High Performance Computing Modernization Program (HPCMP) **FRONTIER**

Award. The Army project is titled "Petascale High Fidelity Simulation of Atomization and Spray/Wall Interactions at Diesel Engine Conditions". The simulations were run on the Garnet Cray XE6 computing platform. The author would also like to thank Drs. Michael Tess and Matthew Kurman for measuring rate-of-injection profiles for this work.

The submitted manuscript has been created by UChicago Argonne, LLC, Operator of Argonne National Laboratory ("Argonne"). Argonne, a U.S. Department of Energy Office of Science laboratory, is operated under Contract No. DE-AC02-06CH11357. The U.S. Government retains for itself, and others acting on its behalf, a paid-up nonexclusive, irrevocable worldwide license in said article to reproduce, prepare derivative works, distribute copies to the public, and perform publicly and display publicly, by or on behalf of the Government. This research was funded by DOE's Office of Vehicle Technologies, Office of Energy Efficiency and Renewable Energy under **Contract No. DE-AC02-06CH11357**. The authors' wish to thank Gurpreet Singh and Leo Breton, program managers at DOE, for their support.

## REFERENCES

- [1] Colket, M., Edwards, T., Williams, S., Cernansky N.P., Miller, D.L., Egolfopoulos, F., Lindstedt, P., Seshadri, K., Dryer, F., Law, C., Friend, D., Lenhert, D., Pitsch, H., Sarofim, A., Smooke, M., Tsang, W. "Development of an Experimental Database and Kinetic Models for Surrogate Jet Fuels," in *45th AIAA Aerospace Sciences and Exhibit, AIAA 2007-770*, 2007.
- [2] Schulz, W.D., "Oxidation Products of a Surrogate JP-8 Fuel", ACS Petroleum Chemistry Division Preprints 37 (1991), pp. 383-392.
- [3] Edwards, T., Maurice, L.W., "Surrogate Mixtures to Represent Complex Aviation and Rocket Fuels," *Journal of Propulsion and Power*, vol. 17, no. 2, pp. 461-466, Mar. 2001.
- [4] Bravo, L., Kurman, M., Kweon, C., Wijeyakulasuriya, S., Senecal, P.K., "Lagrangian Modeling of Evaporating Sprays at Diesel Engine Conditions: Effects of Multi-Hole Injector Nozzle with JP-8 Surrogates", *Proceedings of the 26th Annual Conference of Liquid Atomization and Spray Systems*, Portland, Oregon, May 2014.
- [5] Kurman, M., Bravo, L., Kweon, C., Tess, M., "The Effect of Fuel Injector Nozzle Configuration on JP-8 Sprays at Diesel Engine Conditions", *Proceedings of the 26th Annual Conference of Liquid Atomization and Spray Systems*, Portland, Oregon, May 2014.
- [6] Violi, A., Yan, S., Eddings, E., Sarofim, A.F., Granata, S., Faravelli, T., Ranzi, E., "Experimental formulation and kinetic model for JP-8 surrogate mixtures," *Combustion Science and Technology*, vol. 174, no. 11-12, pp. 399-417, Nov. 2002.
- [7] Montgomery, C.J., Cannon, S.M., Mawid, M.A., Sekar, B., "Reduced Chemical Kinetic Mechanism for JP-8

- Combustion", 40th AIAA Aerospace Sciences Meeting and Exhibit, 14-17 Jan 2002, Reno, Nevada.
- [8] Humer, S., Frassoldati, A., Granata, S., Faravelli, T., Ranzi, E., Seiser, R., K. Seshadri, "Experimental and kinetic modeling study of combustion of JP-8, its surrogates and reference components in laminar non-premixed flows," *Proceedings of the Combustion Institute*, vol. 31, no. 1, pp. 393–400, Jan. 2007.
  - [9] Honnet, S., Seshadri, K., Niemann, U., Peters, N., "A surrogate fuel for kerosene," *Proceedings of the Combustion Institute*, vol. 32, no. 1, pp. 485–492, Jan. 2009.
  - [10] Seshadri, K., Frassoldati, A., Cuoci, A., Faravelli, T., Niemann, U., Weydert, P., Ranzi, E., "Experimental and kinetic modeling study of combustion of JP-8, its surrogates and components in laminar premixed flows," *Combustion Theory and Modeling*, vol. 15, no. 4, pp. 569–583, Aug. 2011.
  - [11] Pitz W., Westbrook, C., "Progress in Chemical Kinetic Modeling for Surrogate Fuels (LLNL-CONF-404514)," in *The 7th COMODIA International Conference on Modeling and Diagnostics for Advanced Engine Systems*, 2008.
  - [12] Issa, R.I., "Solution of the implicitly discretized fluid flow equations by operator splitting", *Journal of Computational Physics*, 40: 62, 1985.
  - [13] Kastengren, A., Powell, C., Liu, Z., Moon, S., Gao, J., Zhang, X., Wang, J., "Axial Development of Diesel Sprays at Varying Ambient Density", *Proceedings of the 22<sup>nd</sup> Annual Conference of Liquid Atomization and Spray Systems*, Cincinnati, Ohio, May 2010.
  - [14] Kastengren, A., Tilocco, F., Powell, C., Manin, J., Pickett, L., Payri, R., Bazyn, T., "Engine Combustion Network (ECN): Measurements of nozzle geometry and hydraulic behavior", *Atomization and Sprays*, vol 22, 12, 2012.
  - [15] Xue, Q., Battistoni, M., Som, S., Quan, S., Senecal, P.K., Pomraning, E., Schmidt, D., "Eulerian CFD modeling of coupled nozzle flow and spray with validation against xray radiography data", *SAE International Journal of Fuels and Lubricants*, (2):2014, doi:10.4271/2014-01425
  - [16] Xue, Q., Battistoni, M., Powell, C.F., Longman, D.E., Quan, S.P., Senecal, P.K., Pomraning, E., Schmidt, D.P., Som, S., "An Eulerian CFD model and X-ray radiography for coupled nozzle flow and spray in internal combustion engines", *International Journal of Multiphase Flow*, vol. 70, pp. 77-88, 2015.
  - [17] Senecal, P., Richards, K., Pomraning, E., Yang, T., Dai, M., McDavid, R.M., Patterson, M.A., Hou, S., Sethaji, T., 2007. A New Parallel Cut-cell Cartesian CFD Code for Rapid Grid Generation Applied to In-cylinder Diesel Engine Simulations. SAE Technical Paper 2007-01-0159.
  - [18] Vallet, A., Burluka, A.A., Borghi, R., 2001. Development of a Eulerian model for the "atomization" of a liquid jet. *Atomization Sprays* 11, 619–642.
  - [19] Zhao, H., Quan, S., Dai, M., Pomraning, E., Senecal, P., Xue, Q., Battistoni, M., Som, S., 2014. "Validation of a three-dimensional internal nozzle flow model including automatic mesh generation and cavitation effects". *J.Eng. Gas Turb. Power* 136, 092603-1.
  - [20] Kastengren, A.L., Tilocco, F.Z., Duke, D., Powell, C.F., Zhang, X., Moon, S., 2014. "Time- resolved X-ray radiography of sprays from engine combustion network Spray A diesel injector", *Atomization and Sprays* 24, 251-272.
  - [21] ECN. Engine Combustion Network ([www.sandia.gov/ecn](http://www.sandia.gov/ecn))
  - [22] Colket, M., Zeppieri, S., Dai, Z., Kim, W., Hollick, H., and Hautman, D., (2013) "Alternative Fuels Modeling for Navy Applications," ONR Contract N00014-12-C-0408, Final Report, June, 2013.

1 DEFENSE TECHNICAL  
(PDF) INFORMATION CTR  
DTIC OCA

2 DIRECTOR  
(PDF) US ARMY RESEARCH LAB  
RDRL CIO LL  
IMAL HRA MAIL & RECORDS  
MGMT

1 GOVT PRINTG OFC  
(PDF) A MALHOTRA

2 DIR USARL  
(PDF) RDRL VTP  
L BRAVO  
C-B M KWEON